

Branched wrinkles in inhomogeneous film-on-substrate systems

Roland Aichele,¹ Badr Kaoui,^{1,2} Falko Ziebert,³ and Walter Zimmermann¹

¹*Theoretical Physics I, University of Bayreuth, Universitätsstrasse 30, D-95447 Bayreuth, Germany*

²*CNRS - Sorbonne University, Université de Technologie de Compiègne, UMR7338 Biomechanics and Bioengineering, F-60203 Compiègne, France*

³*Physikalisches Institut, Albert-Ludwigs-Universität Freiburg, D-79104 Freiburg, Germany*

(Dated: June 25, 2017)

We model the post-buckling behavior of wrinkles in thin solid films supported by inhomogeneous substrates under uniaxial deformation. On homogeneous substrates, the preferred wave vector of the wrinkles points along the stretching direction, which represents an inherent anisotropy, and the wavelength is determined by the elasticities of the film vs. the substrate. In turn, a spatial variation of the substrate elasticity perpendicular to the anisotropy [as recently studied experimentally by B. Glatz *et al.* *Soft Matter* **11**, 3332 (2015)] triggers the formation of branched wrinkle patterns with spatially varying wave numbers. By modeling wrinkling on substrates with either a step-like or linearly ramped variation of stiffness (i.e. elastic modulus), we find in the post-buckling regime a coexistence of many branched wrinkle patterns having different wave numbers and different densities of branching points, and being stable at identical parameters: the selected pattern depends on the initial conditions. The stability range of branched patterns is narrower for smooth compared to steep stiffness changes, and the ordering of the branching points depends on the length scale of the stiffness variation.

I. INTRODUCTION

There is an increasing interest in generating structured surfaces with patterns of sizes down to the nanoscale for various tunable applications. A promising route is to exploit mechanical surface instabilities, leading to wrinkle patterns on top of films supported by elastic substrates [1–5], as shown in Fig. 1. A common model system is obtained as follows, cf. Fig. 1(a): an elastomeric substrate (e.g. PDMS) is stretched in one direction. A thin, stiffer surface layer is then deposited or created (for instance, via oxidation, cf. e.g. Refs. [6, 7]), as marked in blue in Fig. 1(a). Finally, after relaxation of the initial stretch, periodic wrinkles occur at the surface of the sandwiched system. They are oriented perpendicular to the uniaxial stretch direction and their wavelength is determined by the ratio between the bending rigidity of the thin film and the bulk elastic modulus of the substrate.

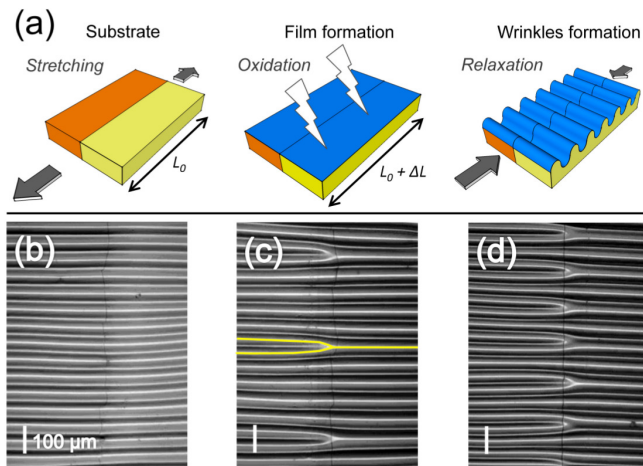


FIG. 1: Part (a) sketches the three steps of creating a thin stiff film (blue) on the top of a substrate and the formation of wrinkles. The substrate may be homogeneous or inhomogeneous (composed of two materials A and B of different elasticities), as sketched. Parts (b), (c) and (d) are experimental micrographs showing wrinkle patterns in such composite systems: in (b) the two parts have the same elastic moduli and wrinkles are straight, (c) and (d) show branched wrinkles, where the branching points (defects) emerge at the border between the different substrates. Parts (b), (c) and (d) modified from [7] - Published by The Royal Society of Chemistry.

The instability towards wrinkling is understood for several elastic systems [8–13]. The post-buckling behavior in film on substrate systems has been in part explored for small system sizes [14–16] and recently secondary buckling

transitions have attracted considerable attention [18, 19, 39]. Much less theoretical analysis is available for wrinkles below these secondary transitions, but in large, spatially extended systems and concerning the possible coexistence of different stable wrinkle states, as occurring in experiments [20]. Wrinkle patterns belong to the universality class of stationary and spatially periodic patterns, being ubiquitous in nature and technology [21–23]. A central property of nonlinear periodic patterns is that – at given parameters – not only a single wave number may be stable, but rather many different wave numbers within the so-called (Eckhaus) stability bands [22–32]. For instance, for the periodic buckling of plates – closely related to the wrinkle system – such bands of stable patterns with different wave numbers have been found [27, 28]. Therefore, for the wrinkle system, as well, stable wave number bands are to be expected, as suggested also from models accounting for hyperelasticity [31, 35]. But this property has not yet been explored systematically for realistic elastic film-substrate models.

The interplay between the just discussed generic wave number variability within stability bands, on the one hand, and spatial parameter variations that influence the wave number, on the other hand, opens many interesting options for pattern competition and design. In fact, anisotropic pattern forming systems that experience slow parameter variations perpendicular to the preferred direction have been recently identified as a new symmetry class in pattern formation [35] that displays rich coexistence scenarios.

For wrinkles, different possibilities exist to modulate the wave number: for instance, spatial variations of the stiffness of either the substrate [7, 35–38] or of the film [6], variations of the topography [39] as well as a non-uniform thickness of the film [40, 41]. Anisotropic loads were also suggested [42]. In the present study, we focus on the case where the substrate stiffness (i.e. the elastic modulus) varies along the direction perpendicular to the anisotropy (determined by the initial stretch). One system considered here is a substrate composed of two parts having different elastic moduli, as indicated in Fig. 1(a) by the orange- and yellow-colored blocks. Experimental micrographs of wrinkle patterns formed on such an inhomogeneous setup are shown in Fig. 1 (b)-(d), cf. [7]: When both parts have the same modulus, this corresponds to the homogeneous case and the wrinkles go straight over the line where the two substrates were glued together, cf. Fig. 1(b). When the two elastic moduli in A and B are different, however, the adopted wavelengths in each part differ as well. Consequently, defects emerge along the matching line between parts A and B to accommodate the change in the wavelength. Increasing the difference in the elasticities [from Fig. 1(c) to (d)], leads to an increase in the density of defects.

In such inhomogeneous anisotropic systems, the interplay of the wave number variability and the parameter variations orthogonal to the wave vector leads to rich coexistence scenarios of periodic patterns: namely, wrinkle patterns of different wave numbers and displaying different numbers of branching points are stable at identical sets of parameters. At least, this was suggested in Ref. [35] for small and smooth harmonic parameter variations. Here, we go beyond this perturbative approach by considering the step-like parameter change just discussed – and as realized in the recent experiments [7] – in Sec. III and in addition linear ramps in the stiffness in Sec. IV, to address the following questions: Will the coexistence scenario between branched and straight patterns, obtained in Ref. [35] for small harmonic variations, prevail for step-like and ramped variations? Will the concept of Eckhaus stability bands [22, 25, 31], established so far for homogeneous systems, be applicable in some generalized manner to inhomogeneous systems? How do the branching points of the wrinkle patterns, cf. Fig. 1(c) and (d), order for step-like or linearly ramped parameters?

II. MODEL FOR WRINKLES IN AN HYPERELASTIC SYSTEM

To describe the wrinkles in parameter modulated systems as shown in Fig. 1(a), we use a model that neglects in-plane film-deformations (i.e. shearing and stretching/compression). The buckling deformation of the film, away from the undeformed base state of the film given by the xy -plane, is described by the field $u(x, y, t)$.

A. Homogeneous model

For a homogeneous substrate the model equation for $u(x, y, t)$ has the form as follows [31, 35]:

$$\rho \partial_t u = - [\kappa_x \partial_x^4 + 2\kappa_{xy} \partial_x^2 \partial_y^2 + \kappa_y \partial_y^4] u - [\mu_x \partial_x^2 + \mu_y \partial_y^2] u - \alpha u - \gamma u^3. \quad (1)$$

Here κ_x , κ_y and κ_{xy} are the three, in general different, bending moduli of the thin film. μ_x and μ_y are the axial forces exerted along x and y directions, respectively. α is the linear elastic modulus of the supporting substrate and γ describes either the nonlinear elastic modulus of the supporting substrate (as occurring for a hyperelastic material) and/or mimics bulk deformations of the thin layer due to the bending. In case the axial forces are different, $\mu_x > \mu_y$, the model is anisotropic and exhibits a preferred direction, here the x -direction.

Onset of wrinkles: The onset of wrinkles can be determined by a linear stability analysis of the undeformed flat film (i.e. of the base state $u = 0$) with respect to small perturbations that have their periodicity along the preferred direction x . For small u the nonlinear term γu^3 in Eq. (1) can be neglected and the remaining linear equation can be solved by $u \propto \exp(\sigma t + i q x)$. The condition for a vanishing growth rate ($\sigma = 0$) yields the equation

$$\kappa_x q^4 - \mu_x q^2 + \alpha = 0, \quad (2)$$

that allows to determine the load μ_x needed to destabilize the base state $u = 0$ by a perturbation of wave number q as a function of the material parameters κ_x and α ,

$$\mu_x(q) = \frac{\kappa_x q^4 + \alpha}{q^2}. \quad (3)$$

Minimizing this expression with respect to q yields the critical wave number q_c , and the critical load $\mu_{x,c}$ at threshold:

$$q_c^4 = \frac{\alpha}{\kappa_x} \quad \text{and} \quad \mu_{x,c} = 2\sqrt{\alpha\kappa_x}. \quad (4)$$

These are classical results and for the wrinkle wavelength at onset [33, 34] holds

$$\lambda_{\text{wrinkle}} = \frac{2\pi}{q_c} \sim \left(\frac{\kappa_x}{\alpha}\right)^{1/4}. \quad (5)$$

Anisotropic Swift-Hohenberg equation. Using the following rescaled parameters,

$$t' = \frac{\mu_x^2}{4\kappa_x q_c^4} t, \quad u' = \frac{2\sqrt{\kappa_x \gamma} q_c^2}{\mu_x} u, \quad (6a)$$

$$x' = \sqrt{\frac{\mu_x}{2\kappa_x q_c^2}} x, \quad y' = \frac{\mu_x}{\sqrt{2\kappa_x \mu_y} q_c^2} y, \quad (6b)$$

Eq. (1) can be mapped into a generalization of the Swift-Hohenberg (SH) equation to anisotropic systems, as introduced in Ref. [31]:

$$\partial_t u = \left[\varepsilon - (q_c^2 + \nabla^2)^2 \right] u - u^3 - [c \partial_y^4 + W \partial_x^2 \partial_y^2] u. \quad (7)$$

Herein the rescaled parameters are the relative distance from the onset of wrinkling,

$$\varepsilon = \left(1 - \frac{\mu_{x,c}}{\mu_x} \right) q_c^4, \quad (8)$$

and two parameters describing the anisotropy

$$c = \frac{\kappa_y \mu_x^2}{\kappa_x \mu_y^2} - 1 \quad \text{and} \quad W = 2 \left(\frac{\kappa_{xy} \mu_x}{\kappa_x \mu_y} - 1 \right). \quad (9)$$

For equal loads $\mu_x = \mu_y$ and equal bending moduli $\kappa_x = \kappa_y = \kappa_{xy} = \kappa$, the anisotropy parameters vanish, $W = c = 0$, and thus Eq. (7) reduces to the original Swift-Hohenberg model for isotropic systems [43].

Performing again a linear stability analysis, now with respect to perturbations of wave numbers q along x and p along y , the base state $u = 0$ becomes unstable beyond the so-called neutral surface $\varepsilon_N(q, p)$, i.e. for

$$\varepsilon > \varepsilon_N(q, p) = (q_c^2 - q^2 - p^2)^2 + c p^4 + W q^2 p^2. \quad (10)$$

For $c > 0$ and $W > 0$ the perturbations with respect to $u = 0$ have largest growth rate at the wave vector $\mathbf{q} = (q, p) = (q_c, 0)$, i.e. its preferred direction is the x -direction [31].

B. Inhomogeneous model

Eq. (4) indicates that position-dependent elastic parameters may cause a position-dependent critical wave number q_c and critical load $\mu_{x,c}$. Obviously, the position-dependent q_c is responsible for the formation of branched wrinkle patterns shown in Fig. 1. A position-dependent $\mu_{x,c}$ only implies that in different areas of the composite system wrinkles form at different loads (namely, first in the regions where the substrate is softer). Although this obviously does not impede the effects we aim at, cf. the experiments shown in Fig. 1, it makes the generic behavior we want to address less transparent. Therefore, to highlight the emergence of multiple solutions (by wavelengths and number of defects, i.e. branching points) and the interplay between the two parts composing the system, we focus on the simpler following case: let us consider systems with steep variations in the material properties, as sketched in Fig. 1(a), and denote the two parts by A and B . By appropriate choices of the bulk elasticities of the substrates, α_A and α_B , and the isotropic bending moduli, κ_A and κ_B , of the two parts it is possible to obtain wrinkles that have different preferred wave numbers in the two parts at the onset, but equal critical load (for instance, if one wants $q_{c,A} = 1$ and $q_{c,B} = q_B$ and equal threshold, one can use $\kappa_A = \alpha_A$, $\kappa_B = \kappa_A q_B^2$ and $\alpha_B = \alpha_A / q_B^2$). The fact that ε , c and W are different in the two parts influence the effects only quantitatively (especially for the two latter: as long as c , W stay both larger than zero, the anisotropy prevails and they otherwise do not change the behavior).

Having identified the position-dependent wave number as the main effect for the occurrence of branched wrinkle patterns, we generalize the model equation (7) by keeping the control parameter ε uniform and by allowing a continuous y -dependent wave number $q_0(y)$ as proposed in Ref. [35]:

$$\partial_t u = \left[\varepsilon - (q_0^2(y) + \nabla^2)^2 \right] u - u^3 - [W \partial_x^2 \partial_y^2 + c \partial_y^4] u - 2(\partial_y u) \partial_y [q_0^2(y)] - u \partial_y^2 [q_0^2(y)]. \quad (11)$$

In the following, we choose fixed anisotropy parameters $c = W = 0.5$, that leads to the formation of straight wrinkles oriented perpendicular to the x -direction [31]. We study this inhomogeneous system numerically using a pseudo-spectral (Fourier-based) method in a two-dimensional domain of size $L_x \times L_y$ with periodic boundary conditions. L_x is chosen to be large to allow the emergence of wrinkles with a large variety of wave numbers. L_y also has to be chosen sufficiently large to be able to observe branching, cf. the discussion in the next section. We consider both rapid changes of $q_0(y)$ [44] as well as smooth linear ramps.

III. WRINKLES IN SYSTEMS WITH SHARP PARAMETER VARIATIONS

Branched wrinkles, as shown in Figs. 1(c) and 1(d), require sufficiently wide regions A and B . The related critical width $L_{y,c}$ is determined in Sec. III A. After briefly recalling the stability range of straight wrinkles (the *Eckhaus band*) in a *homogeneous* anisotropic system in Sec. III B, the stability range of both straight and branched wrinkles in the *inhomogeneous* composite A - B -system is studied in Sec. III C.

A. Minimal width needed for branched wrinkles

Branched wrinkle patterns can indeed be obtained from Eq. (11) for sufficiently different wave number values $q_{0,A}$ and $q_{0,B}$ in the two parts A and B . Nevertheless, as the spatial extension of a branching defect is large at small values of the control parameter ε , branching occurs in such composite systems only for a sufficiently large width in the lateral (here y -)direction. The critical width $L_{y,c}$ – scaled by the characteristic wrinkle wavelength $\lambda_{0,A}$ in the region A – that is needed for the occurrence of branching points is shown as a function of ε in Fig. 2. In this example, we chose the wave number combination $q_{0,A} = 1$ and $q_{0,B} = 0.833$ in A and B , respectively. The system's length was chosen to be $L_x = 72\lambda_{0,A}$ with $\lambda_{0,A} = 2\pi/q_{0,A} = 2\pi$. For $L_y < L_{y,c}(\varepsilon)$ only transient defects may emerge immediately after starting the simulation (as initial condition, small noise was added to a flat surface). These transient defects quickly disappear in favor of finally perfectly straight unbranched wrinkles. However, by enlarging $L_y > L_{y,c}(\varepsilon)$, branched patterns with defects become stable. $L_{y,c}$ is found to be a decreasing function of ε , because the extension of the branching defect decreases with increasing ε . Accordingly, for a given width L_y one has to increase ε beyond a critical value to obtain branched wrinkle patterns.

It should be noted that this result has been obtained using periodic boundary conditions in y , i.e. in fact we studied an infinite periodic array of alternating A and B regions. The qualitative behavior of $L_{y,c}(\varepsilon)$, however, will be the same for a finite system.

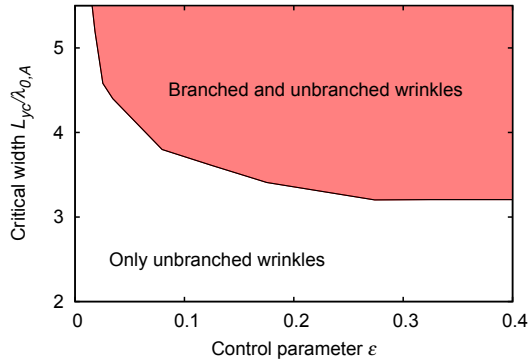


FIG. 2: The critical width $L_{yc}/\lambda_{0,A}$ above which stable branched wrinkles form as a function of the control parameter ϵ . The wave number difference $\Delta q_0 = q_{0,A} - q_{0,B} = 1 - 0.833 = 0.167$ was used and a system size in x -direction of $L_x = 96 \times \lambda_{0,A}$.

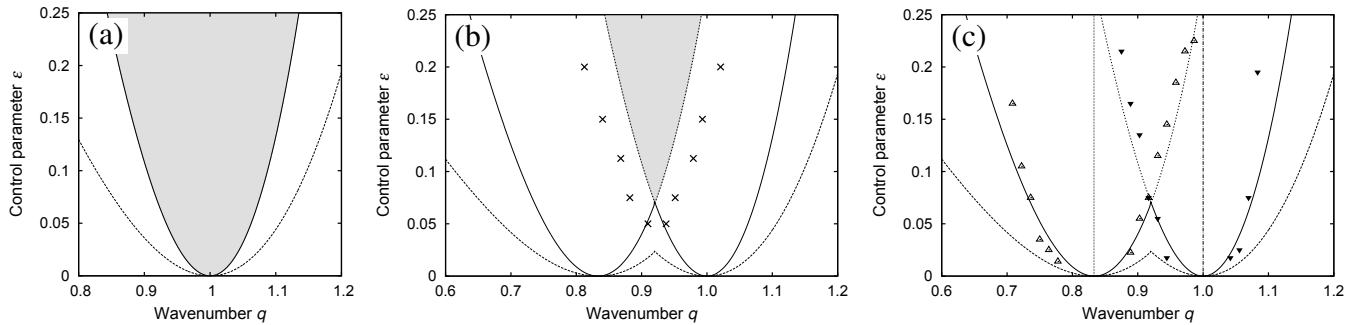


FIG. 3: (a) The neutral curve (dashed line) obtained by Eq. (12) and the Eckhaus stability curve (solid line) obtained by Eq. (13) for a homogeneous system with $q_0 = 1$. (b) The neutral and the Eckhaus curves for two homogeneous systems with intrinsic wave numbers $q_{0,A} = 1$ and $q_{0,B} = 0.8333$ (uncoupled case). When Eq. (11) is studied numerically with the critical wave number varying along the y -direction rapidly between $q_{0,A}$ and $q_{0,B}$, one finds stable straight wrinkle patterns for control parameters ϵ above the crosses. (c) The stability range of numerically obtained branched solutions, cf. those shown in Fig. 4(b),(c). A wide range of stable wave numbers out of one of the two Eckhaus-bands (of the uncoupled system) coexist with the wave number q_A (q_B) in the complimentary area: wave numbers between the empty triangles are all stable in region B when $q_{0,A} = 1$; and wave numbers between the filled triangles are stable in region A , when $q_{0,B} = 0.833$. System size: $L_x = 72\lambda_{0,A}$ and $L_y = 20\lambda_{0,A}$.

B. Stability of straight wrinkles

Wrinkles in homogeneous systems orient themselves perpendicularly to the preferred direction of the uniaxial initial stretch. By symmetry they belong to the class of stationary and spatially periodic patterns in two-dimensional anisotropic systems, whereof an early and well explored representative of this class is electroconvection in nematic liquid crystals [22, 48–50]. As has been established for this class [31], patterns can grow for wave vectors within finite regions, centered around the critical wave vector: for the anisotropic model, Eq. (7), this happens beyond the neutral surface, given by Eq. (10), around $\mathbf{q} = (q_0, 0)$.

Restricting the neutral surface to the direction along the preferred axis, the neutral curve $\epsilon_N(q)$ follows,

$$\epsilon_N(q) = (q_0^2 - q^2)^2, \quad (12)$$

which is traced as the dashed line in Fig. 3(a). Hence for a given control parameter value ϵ , all perturbations with wave numbers fulfilling $\epsilon > \epsilon_N(q)$ will grow exponentially.

Which wrinkle wave number q – out of the permitted range beyond the neutral curve $\epsilon_N(q)$ – will finally be selected? This is determined by the prevailing nonlinearities, and also depends on the initial conditions. Importantly, *not necessarily* the periodic state with the wave number $q = q_0$ that initially grows fastest (and that also corresponds to the minimum of the functional from which equation (7) can be derived, see [31, 35]) will be realized. In fact, it is easy to show that any wrinkle pattern with wave number out of the grey range in Fig. 4(a) is itself *linearly stable*

[22, 23, 31]. The solid curve in Fig. 4(a) bounding the stability region of the periodic states is the so-called Eckhaus stability boundary [22, 24, 25] and is given for model Eq. (7) close to onset by

$$\varepsilon_E(q) = 3\varepsilon_N(q) = 3(q_0^2 - q^2)^2. \quad (13)$$

Consequently, for each value of the control parameter ε , a multiplicity of stable coexisting periodic states is possible in the weakly nonlinear regime beyond threshold. Similar finite width Eckhaus stability-bands for periodic nonlinear states have been found in many systems, see e.g. [22, 25–32]. The full two dimensional stability areas in the (q, p) -plane for the homogeneous model Eq. (7) can be found in Ref. [31].

C. Coexistence of straight and branched wrinkles

Considering the homogeneous model given by Eq. (7), but for two different preferred wave numbers $q_{0,A} = 1$ and $q_{0,B} = 0.833$, one obtains close to threshold for each preferred wave number a neutral curve (cf. the dashed lines) and an Eckhaus curve (solid lines): centered around $q_{0,A}$ and $q_{0,B}$, respectively, as shown in Fig. 3(b). This corresponds to the situation of an inhomogeneous system, where the two parts A and B are uncoupled. In this case, one expects straight stripes spanning the whole system (i.e. both region A and B) to be stable, if their wave numbers lie in the grey region, defined by the overlap of the Eckhaus stability regions.

A real A - B -system will be coupled – in case of wrinkles, elastically. If the inhomogeneous model given by Eq. (11) is studied with the preferred wave number $q_0(y)$ changing rapidly from $q_{0,A}$ to $q_{0,B}$, the range of stable straight stripes becomes even larger than for the uncoupled case: they are stable beyond the crosses shown in Fig. 3(b). If the lateral width of the system, L_y , is decreased, the stability range of straight stripes in the composed system becomes even broader. In turn, upon increasing L_y , their stability range approaches the grey range obtained for the uncoupled system. An example of a stable straight wrinkle pattern with a wave number $q_{0,B} < q < q_{0,A}$ spanning the whole system is given in Fig. 4(a).

In addition to straight wrinkles, the inhomogeneous coupled system displays branched wrinkles as shown in Fig. 4 (b) and (c). Importantly, also in this case the wave numbers in the two regions are not strictly fixed, but can be picked up out of whole bands. The system can therefore exhibit – at an identical parameter set – the following intricate coexistence scenarios: (I) coexistence of straight wrinkles of different wave number beyond the crosses in Fig. 3(b), (II) coexistence of straight wrinkles and branched patterns in the same range beyond the crosses, as well as (III) coexistence of branched wrinkles of different wave numbers and hence displaying different numbers of branching points per area in some larger region beyond the Eckhaus curves of the uncoupled system.

The coexistence of different branched wrinkles is characterized in further detail in Fig. 3(c), where we address the following situation: as initial condition, we have chosen a periodic solution with the intrinsic wave number $q_{0,A} = 1$ ($q_{0,B} = 0.833$) in the region A (the region B) and in the complementary area any periodic solution out of the Eckhaus stable band of the uncoupled system. Which combinations will then be stable in the coupled system? Fig. 3(c) shows

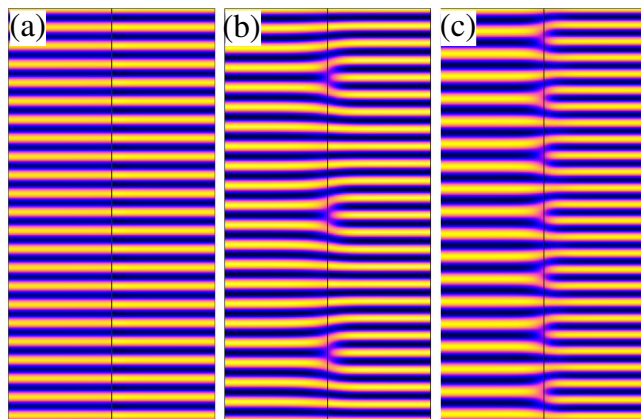


FIG. 4: Three patterns are shown, which are stable solutions of Eq. (11) for the case of a rapid wave number variation. They all have been obtained at the identical parameter set $\varepsilon = 0.1$, $q_{0,A} = 1$ and $q_{0,B} = 0.833$, but for different initial conditions. Panel (a) shows a straight wrinkle pattern with wave number $q_A = q_B = 0.93$. The two branched patterns (b) and (c) are composed of wave numbers $q_A = 1$ and $q_B = 0.875$ and $q_A = 1.065$ and $q_B = 0.764$, respectively. Shown are cuts out of a larger computational domain with $L_x = 72 \lambda_{0,A}$, $L_y = 20 \lambda_{0,A}$ and periodic boundary conditions.

that a wide range of stable wave numbers out of one of the two Eckhaus-bands of the uncoupled system coexist with the fixed wave number in the complimentary area: wave numbers between the empty triangles are all stable in region B , when $q_{0,A} = 1$. In turn, wave numbers between the filled triangles are stable in region A , when $q_{0,B} = 0.833$.

On the basis of this insight, one can imagine preparing a great variety of branched wrinkle patterns by choosing appropriate initial configurations. This behavior, found here numerically for a step-like varying $q_0(y)$ agrees qualitatively with the behavior obtained for small, smooth sinusoidal variations of $q_0(y)$ in Ref. [35]. In experiments the onset of wrinkles in general may be different in the areas A and B (cf. the discussion in section II B) but qualitatively similar scenarios are expected.

IV. RAMPED PARAMETER VARIATIONS

The coexistence of a whole family of different branched wrinkle patterns in a wide region of parameter space, and the coexistence of non-branched and branched patterns in a smaller region, is a generic and robust phenomenon. It has been found for small, smooth harmonic variations of $q_0(y)$ in Ref. [35] and, as described in the previous section, for rapid variations between two constant values $q_{0,A}$ and $q_{0,B}$. In the latter case, the branching points are located near the rapid parameter change between parts A and B , cf. Fig. 1 and 4. Recently, interesting gradient elastomeric materials have been synthesized [37], with the elastic modulus varying linearly in one spatial direction. Wrinkling on such substrates has been studied, but with the elasticity varied along the direction of the initial stretch [38], not yet perpendicularly. This leads us to address the following questions: What is the spatial order of the branching points when $q_0(y)$ is linearly ramped – perpendicular to the anisotropy – between two constant values $q_{0,A}$ and $q_{0,B}$? And how will the stability range of the branched patterns be affected by such a smooth ramping, compared to the rapid variation just discussed?

Fig. 5(a) displays the imposed wave number ramp $q_0(y)$ between $q_{0,A} = 1$ and $q_{0,B} = 0.667$ with a ramp width $\delta = 10\lambda_{0,A}$ and a slope of $\Delta q/\delta$. By solving Eq. (11) numerically for such ramped q -variations and different initial conditions, we find, again at identical parameter sets, either regularly or rather irregularly ordered branching patterns of wrinkles as shown in Figs. 5(b) and (c). Similar branching point orderings have been observed experimentally on substrates with a smooth gradient in the elastic modulus, cf. Ref. [40] and the supplementary material of Ref. [7]. In each pattern configuration, the pattern locally adopts different wave numbers along the y -direction: Fig. 5(d) shows possible local wave number distributions (blue lines), while the grey region shows the range of the ramp.

Similar as for the stability diagram in Fig. 3(c) for the rapid, step-like variation, one may choose now as an initial condition in region A (region B) the wave number $q_{0,A}$ ($q_{0,B}$) at the center of the neutral curve and in the complementary area a wave number out of the Eckhaus stability range corresponding to the uncoupled system. The resulting stable branched patterns with different wave numbers outside the ramped range is shown in Fig. 6 for a wave number ramp of width $\delta = 10\lambda_{0,A}$ and for a large system size, $L_x = 72\lambda_{0,A}$ and $L_y = 80\lambda_{0,A}$. If a pattern with $q_{0,A} = 1$ ($q_{0,B} = 0.833$) is chosen in area A (B), then all combinations with patterns having a wave number in area B (A) between the open (filled) triangles are stable. Therefore, in the presence of a ramp between constant preferred wave numbers, we recover the same generic coexistence scenario of a large family of different branched patterns, with two representatives shown in Fig. 5(b) and (c).

The result in Fig. 6 can be compared with the one in Fig. 3(c), implying that the range of stable branched patterns is substantially smaller when $q_0(y)$ is ramped between area A and B than for a stepwise variation. Namely, in each of both cases shown in Fig. 6 the outside half of the Eckhaus-stability band of the uncoupled system is destabilized. Interestingly, this restricting effect of a ramp on the range of stable wave numbers of patterns (here the branched patterns) in our two dimensional system is similar to results obtained for ramps in quasi one-dimensional pattern forming systems [29, 45–47]. In these works, the so-called ‘weak pinning’, corresponding to a non-smooth change of the parameters, is widening the wave number range of stable patterns, similar as the step-like change does here when compared to the smooth ramp.

The ramp width affects also the ordering of branching points as shown in Fig. 7. The adopted local wave number (for different initial conditions) displays several ‘layers’ of branching defects as a function of the ramp width δ . For small δ (tending to zero) the branching points are attracted to the line located at the interface separating the two media (cf. sec. III). Upon increase of δ the mean distance between the branching points increases and they start to rearrange into a zig-zag order. Upon further increasing δ one observes, that the branching points arrange along several lines perpendicular to the wave-number ramp, as indicated for instance in Fig. 7(e) by the steps in the wave number. Thus, increasing the ramp’s width (and hence decreasing the slope of the wave number variation) allows for the emergence of additional locally adopted wave numbers. In the limit of very small slopes the mean distance in y direction between branching points becomes large and less ordered and the wave-number steps decrease during its variation from $q_{0,A}$ to $q_{0,B}$.

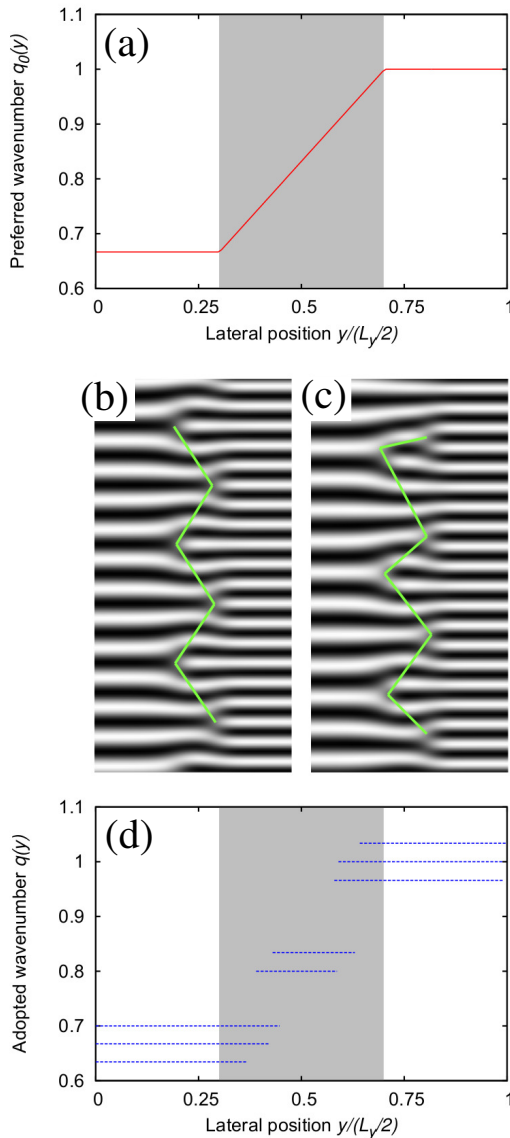


FIG. 5: (a) Shown is a ramp in the imposed wave number $q_0(y)$, i.e. a linear variation from $q_{0,B}$ to $q_{0,A}$. Part (b) [part (c)] shows a wrinkle pattern with a regular [irregular] zig-zag ordering of the branching points at the location of the ramp. (d) The adopted wave numbers in the three respective regions ($q_{0,B}$, ramp, and $q_{0,A}$) as obtained from 6 simulations with different initial conditions.

V. DISCUSSION AND CONCLUSIONS

We have modeled generic effects of wrinkle formation in inhomogeneous film-on-substrate systems under axial loads. Our modeling is related to recent experiments, where material parameters of the film and/or the substrate vary along the direction perpendicular to the uniaxial load direction [7, 36]. In addition, such systems belong to a recently identified new symmetry class of pattern formation [35], that are anisotropic in one direction and inhomogeneous in the direction orthogonal to the anisotropy.

When a film-on-substrate system is composed of two different substrate materials, A and B , that alternate perpendicular to the loading direction and prefer different wave numbers (due to, e.g., different elasticities), then the emerging wrinkle patterns may display branching points located at the region where the materials match. While this observation is intuitive – the system is frustrated and has to accommodate to the two different intrinsic wave numbers of the regions A and B – the following observations are quite surprising: (i) straight wrinkles without branching points and with different wave numbers coexist at a single parameter set in a certain range in the plane spanned by

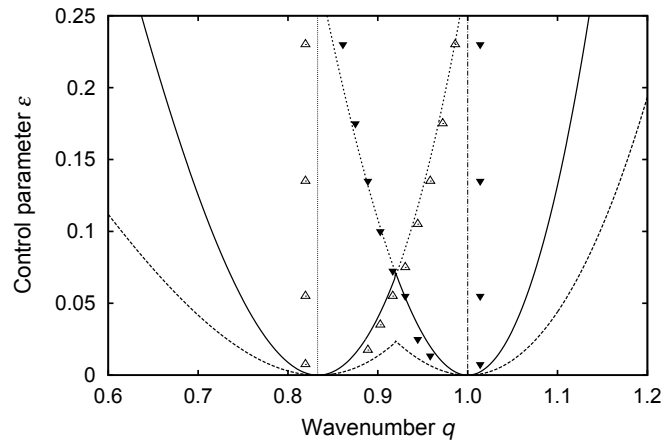


FIG. 6: This stability diagram is analogous to Fig. 3(c), but for a linear ramp-variation of $q_0(y)$ with width $\delta = 10\lambda_{0,A}$ instead of a rapid, step-like one. The dashed lines are the neutral curves and the solid lines the Eckhaus curves for the uncoupled systems centered at $q_{0,B} = 0.833$ and $q_{0,A} = 1$, respectively. The filled (open) triangles indicate the wave number range out of the Eckhaus curve centered around $q_{0,A} = 1.000$ ($q_{0,B} = 0.833$) that yield stable branched solutions when combined with a fixed $q_{0,B}$ ($q_{0,A}$) in the complementary part. System size: $L_x = 72\lambda_{0,A}$ and $L_y = 80\lambda_{0,A}$.

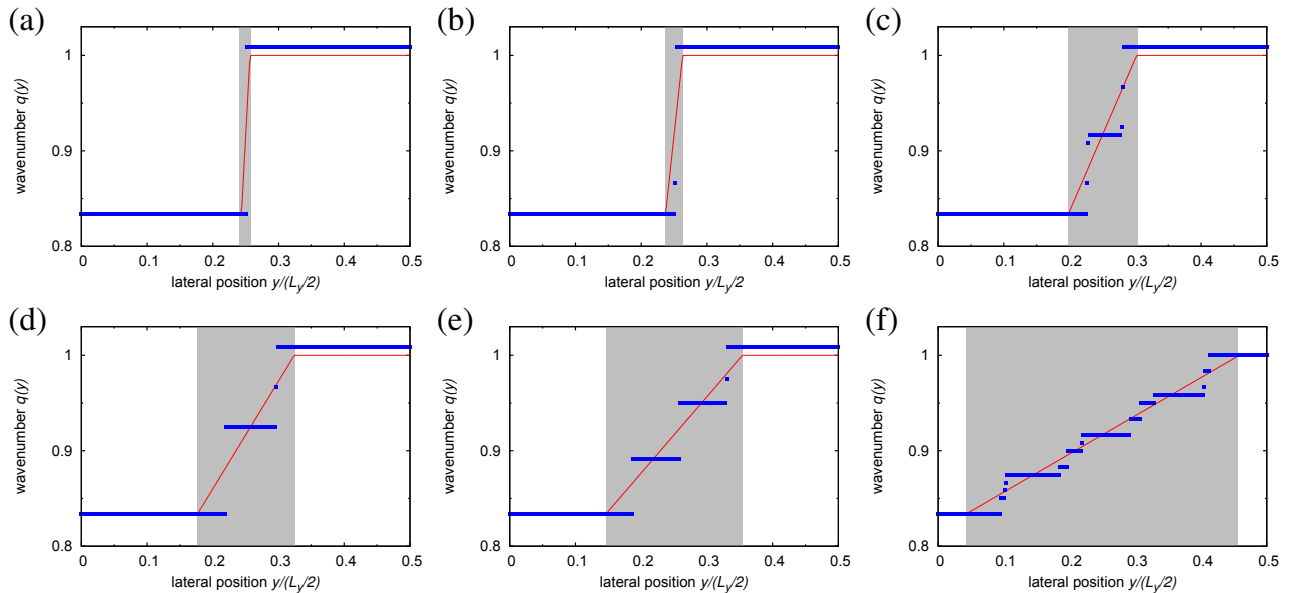


FIG. 7: Studied is the dependence of the adopted wave numbers on the width of the ramp (shaded range). The red solid lines indicate the imposed preferred wave number $q_0(y)$ and the wave numbers locally adopted by the system for different initial conditions are shown by the blue lines. The ramp width varies from (a) to (f) as $\delta = 6.54, 13.09, 52.36, 74.05, 104.72$ and 209.44 . Upon increase of δ , additional 'effective layers' of branching points occur, visible by additional jumps connecting additional q -plateaus in the locally adapted wave numbers. Other parameters: $\varepsilon = 0.08$, $L_x = 120\lambda_{0,A}$, $L_y = 80\lambda_{0,A}$, $\Delta q_c = 0.167$.

the control parameter (related to the stretch) and the wave number of the pattern. Moreover, (ii) in the same region straight wrinkles coexist with branched patterns and (iii) in an even larger region, branched wrinkles of different defect densities and different wave numbers in the two regions A and B coexist.

This seemingly puzzling and very rich coexistence scenario is in fact a generalization of the Eckhaus stability bands known from homogeneous pattern forming systems, which we used here to interpret our findings. Namely, spatially periodic, nonlinear stripe-patterns – in the here-considered system the wrinkles – are not only stable at a unique wave number (the preferred wave number q_0 of maximal linear growth rate), but rather within the so-called Eckhaus stability bands that have finite widths [22, 24, 25]. This well known concept, verified in several homogeneous pattern forming systems [26–32], the closest to the wrinkling system being the buckling of plates [27, 28], is here proven useful

also in its generalization to inhomogeneous and anisotropic systems.

Moreover, these coexistence scenarios – occurring in wide ranges of the parameter space – are also very robust with respect to the specific form of the spatial variations of the preferred wave number $q_0(y)$: they occur not only for smooth harmonic parameter modulations, where the modulational effects close to threshold have been described by a new generic amplitude equation, cf. [35]. We here have shown that they are also encountered for larger step-like, as well as for linearly ramped parameter variations. In addition we found that the range of coexistence of the branched patterns is smaller for linear ramps than for step-like variations. Note that similar changes of the width of the stability bands as a function of the smoothness of the perturbation have been found in quasi-one dimensional systems, studying so-called pinning ramps [29, 45–47].

The described behavior is important for the interpretation of experiments, when material parameters vary along the direction perpendicular to the stretching either in the substrate [7] or in the film [6]. Besides influencing the local wave number, spatial parameter variations in film-on-substrate systems may also change the local critical loads above which the wrinkles form. Consequently, the latter will also influence the described coexistence on the quantitative level, but presumably not qualitatively.

Beyond the wrinkling system, we would like to mention that the homogeneous model equation (7) applies to anisotropic systems displaying stationary periodic patterns in general [31]. In fact, it was originally motivated and used to study certain aspects of electroconvection in planarly aligned nematic liquid crystals, one of the major representatives of anisotropic, dissipative pattern forming systems [31, 48–50]. Consequently, the results obtained in this work for the *inhomogeneous* model equation (11) will also apply to, for instance, planarly aligned electroconvection in nematic liquid crystals where the height of the convection cell (determining the wave number of the convection rolls) varies along the direction perpendicular to the orientation of the nematic director (cf. Ref. [35]).

In the case of equal (or nearly equal) loading in Eq. (1) this pattern forming system may give rise for rapid parameter variations to interesting selection phenomena similar as recently described in Ref. [51], in the case spatial modulations of the stiffness in the thin film, cf. Ref. [6], to pattern orientations as in Refs. [52, 53] or in the case of an irregularly varying stiffness to localized patterns [54].

-
- [1] J. Genzer and J. Groenewold, *Soft matter with hard skin: From skin wrinkles to templating and material characterization*, *Soft Matter* **2**, 310 (2005).
 - [2] J. Y. Chung, A. J. Nolte and C. M. Stafford, *Surface Wrinkling: A Versatile Platform for Measuring thin Film Properties*, *Adv. Mat.* **23**, 349 (2011).
 - [3] B. Li, Y.-P. Cao, X.-Q. Feng and H. Gao, *Mechanics of morphological instabilities and surface wrinkling in soft materials: a review*, *Soft Matter* **8**, 5728 (2012).
 - [4] C.-M. Chen and S. Yang, *Wrinkling instabilities in polymer films and their applications*, *Polym. Int.* **61**, 1041 (2012).
 - [5] H. Y. Bae, S. Bae, C. Park, S. Han, J. Kim, L. N. Kim, K. Kim, S. H. Song, W. Park and S. Kwon, *Biomimetic Microfingerprints for Anti-Counterfeiting Strategies*, *Adv. Mat.* **27**, 2083 (2015).
 - [6] J. Weng, B. Li, Y.-P. Cao, X.-Q. Feng and H. Gao, *Wrinkling micropatterns regulated by a hard skin layer with a periodic stiffness distribution on a soft material*, *Appl. Phys. Lett.* **108**, 021903 (2016)
 - [7] B. A. Glatz, M. Tebbe, B. Kaoui, R. Aichele, C. Kuttner, A. E. Schedl, H.-W. Schmidt, W. Zimmermann and A. Fery, *Hierarchical line-defect patterns in wrinkled surfaces*, *Soft Matter* **11**, 3332 (2015).
 - [8] J. Groenewold, *Wrinkling of plates coupled with soft elastic media*, *Physica A* **298**, 32 (2001).
 - [9] Z. Huang, W. Hong and Z. Suo, *Evolution of wrinkles in hard films on soft substrates*, *Phys. Rev. E* **70**, 030601 (2004).
 - [10] Z. Y. Huang, W. Hong and Z. Suo, *Nonlinear analyses of wrinkles in a film bonded to a compliant substrate*, *J. Mech. Phys. Solids* **53**, 2101 (2005).
 - [11] E. Cerda, K. Ravi-Chandar, L. Mahadevan, *Thin films: Wrinkling of an elastic sheet under tension*, *Nature* **419**, 579 (2002).
 - [12] J. Huang, B. Davidovitch, C. D. Santangelo, T. P. Russell, N. Menon, *Smooth Cascade of Wrinkles at the Edge of a Floating Elastic Film*, *Phys. Rev. Lett.* **105**, 038302 (2010).
 - [13] B. Audoly, *Localized buckling on floating elastica*, *Phys. Rev. E* **84**, 011605 (2011).
 - [14] X. Chen and J. W. Hutchinson, *Herringbone buckling patterns of compressed thin films on compliant Substrates*, *J. Appl. Mech.* **71**, 597 (2004).
 - [15] B. Audoly and A. Boudaoud, *Buckling of a stiff film bound to a compliant substrate - Part I: Formulation, linear stability of cylindrical patterns, secondary bifurcations*, *J. Mech. Phys. Solids* **56**, 2401 (2008).
 - [16] S. Cai, D. Breid, A. J. Crosby, Z. Suo and J. W. Hutchinson, *Periodic pattern and energy states of buckled films on compliant substrates*, *J. Mech. Phys. Solids* **59**, 1094 (2011).
 - [17] H. Vandeparre, M. Pineirua, F. Brau, B. Roman, J. Bico, C. Gay, W. Bao, C. N. Lau, P. M. Reis, P. Damman, *Multiple-length-scale elastic instability mimics parameteric resonance of nonlinear oscillators*, *Nature Phys.* **7** 56 (2010).
 - [18] F. Brau, P. Damman, H. Diamant, T. A. Witten, *Wrinkle to Fold transition: Influence of the substrate response*, *Soft Matter* **9** 8177 (2013)

- [19] S. Budday, S. Kuhl, J. W. Hutchinson, *Period-doubling and period-tribbling in growing bilayered systems*, *Phil. Mag.* **95**, 3208 (2015)
- [20] T. Ohzono and M. Shimomura, *Effect of thermal annealing and compression on the stability of microwrinkle patterns*, *Phys. Rev. E* **72**, 025203(R) (2005).
- [21] P. Ball, *The Self-Made Tapestry: Pattern Formation in Nature*, (Oxford Univ. Press, Oxford, 1998).
- [22] M. C. Cross and P. C. Hohenberg, *Pattern formation outside of equilibrium*, *Rev. Mod. Phys.* **65**, 851 (1993).
- [23] M. C. Cross and H. Greenside, *Pattern Formation and Dynamics in Nonequilibrium systems* (Cambridge Univ. Press, Cambridge, 2009).
- [24] V. Eckhaus, *Studies in Nonlinear Stability Theory* (Springer, Berlin, 1965).
- [25] L. Kramer and W. Zimmermann, *On the Eckhaus instability for spatially periodic patterns*, *Physica D* **16**, 221 (1985).
- [26] M. Lowe and J. P. Gollub, *Pattern Selection near the Onset of Convection: The Eckhaus Instability*, *Phys. Rev. Lett.* **55**, 2575 (1985).
- [27] M. Boucif, J. E. Wesfreid and E. Guyon, *Role of boundary conditions on the mode selection in a buckling instability*, *J. Physique Lett.* **45**, 413 (1984).
- [28] W. Zimmermann and L. Kramer, *Wavenumber restriction in the buckling instability of a rectangular plate*, *J. Phys. (Paris)* **46**, 343 (1985).
- [29] M. A. Dominguez-Lerma, D. S. Cannell and G. Ahlers, *Eckhaus boundary and wave-number selection in rotating Couette-Taylor flow*, *Phys. Rev. A* **34**, 4956 (1986).
- [30] H. Riecke and H. G. Paap, *Stability and wave-vector restriction of axisymmetric Taylor vortex flow*, *Phys. Rev. A* **33**, 547 (1986).
- [31] W. Pesch and L. Kramer, *Nonlinear analysis of spatial structures in two-dimensional anisotropic pattern forming systems*, *Z. Phys. B* **63**, 121 (1986).
- [32] V. Weith and A. Krekhov and W. Zimmermann, *Stability and Orientation of Lamellae in Diblock-Copolymer Films*, *J. Chem. Phys.* **129**, 054908 (2013).
- [33] E. Cerda and L. Mahadevan, *Geometry and physics of wrinkling*, *Phys. Rev. Lett.* **90**, 074302 (2003).
- [34] In film on substrate systems for the linear elastic modulus α also are more adequate description has been developed with a linear dependence of α on the wrinkle-wavenumber [8]: $\lambda_{\text{wrinkle}} = \frac{2\pi}{q_c} \sim \left(\frac{\kappa_{\text{e}}}{\alpha}\right)^{1/3}$. For the competition and the coexistence of patterns with different wavenumber this leads only to small quantitative changes.
- [35] B. Kaoui, A. Guckenberger, A. P. Krekhov, F. Ziebert and W. Zimmermann, *Coexistence of Stable Branched Patterns in Anisotropic Inhomogeneous Systems*, *New J. Phys.* **17**, 103015 (2015).
- [36] Y. Ni, D. Yang and L. He, *Spontaneous wrinkle branching by gradient stiffness*, *Phys. Rev. E* **86**, 031604 (2012).
- [37] K. U. Claussen, R. Giesa, T. Scheibel and H.-W. Schmidt, *Learning From Nature: Synthesis and Characterization of Longitudinal Polymer Gradient Materials Inspired by Mussel Byssus Threads*, *Macromol. Rap. Comm.* **33**, 206 (2012).
- [38] K. U. Claussen, M. Tebbe, R. Gisa, A. Schweikart, A. Fery and H.-W. Schmidt, *Towards tailored topography: facile preparation of surface-wrinkled gradient poly(dimethyl siloxane) with continuously changing wavelength*, *RCS Adv.* **2** 10185 (2012).
- [39] H. Vandeparre and M. Pineirua and F. Brau and B. Roman and J. Bico and C. Gay and W. Bao and C. N. Lau and P. M. Reis and P. Damman, *Wrinkling Hierarchy in Constrained Thin Sheets from Suspended Graphene to Curtains*, *Phys. Rev. Lett.* **106**, 224301 (2011).
- [40] J. Yin and X. Chen, *Elastic buckling of gradient thin films on compliant substrates*, *Philos. Mag. Lett.* **90**, 423 (2010).
- [41] S. Yu, Y. Ni, L. He and Q.-L. Ye, *Tunable Formation of Ordered Wrinkles in Metal Films with controlled Thickness Gradients Deposited on Soft Elastic Substrates*, *ACS Appl. Mater. Interfaces*, **7**, 5160 (2015).
- [42] Y.-C. Chen and A. J. Crosby, *Wrinkling of inhomogeneously strained thin polymer films*, *Soft Matter* **9**, 43 (2013).
- [43] J. Swift and P. C. Hohenberg, *Hydrodynamics fluctuations at the convective instability*, *Phys. Rev. A* **15**, 319 (1977).
- [44] For step-like changes, in principle matching conditions at the step dividing A and B have to be taken into account. However, with a Fourier method this is not needed and the Gibbs phenomenon (ringing) does not pose problems since high modes are damped in the used model. In addition we have checked that a steep linear interpolation in $q_0(y)$, as well as a steep tanh-profile, between regions A and B yield the same result as the Fourier code.
- [45] L. Kramer, E. Ben-Jacob, H. Brand and M. C. Cross, *Wavelength selection in systems far from equilibrium*, *Phys. Rev. Lett.* **49**, 1891 (1982).
- [46] D. S. Cannell, M. A. Dominguez-Lerma and G. Ahlers, *Experiments on Wave Number Selection in Rotating Couette-Taylor Flow*, *Phys. Rev. Lett.* **50**, 1365 (1983).
- [47] H. Riecke, *Pattern Selection by Weakly Pinning Ramps*, *Europhys. Lett.* **2**, 1 (1986).
- [48] E. Bodenschatz, W. Zimmermann, and L. Kramer, *On electrically driven pattern-forming instabilities in planar nematics*, *J. Phys. (Paris)* **49**, 1875 (1988).
- [49] S. Kai and W. Zimmermann, *Pattern Dynamics in the Electrohydrodynamics of Nematic Liquid Crystals*, *Prog. Theor. Phys. Suppl.* **99**, 458 (1989).
- [50] L. Kramer and W. Pesch, *Convection instabilities in nematic liquid crystals*, *Ann. Rev. Fluid Mech.* **27**, 515 (1995).
- [51] L. Rapp, F. Bergmann and W. Zimmermann, *Pattern orientation in finite systems without boundaries*, *EPL* **113**, 28006 (2016).
- [52] Y. Mau, A. Hagberg and E. Meron, *Spatial Periodic Forcing Can Displace Patterns It Is Indented to Control*, *Phys. Rev. Lett.* **109**, 034102 (2012).
- [53] G. Freund, W. Pesch and W. Zimmermann, *Rayleigh-Bénard convection in the presence of spatial temperature modulations*,

- J. Fluid Mech. **673**, 318 (2011).
- [54] W. Zimmermann, M. Sesselberg and F. Petruccione, *Effects of disorder in Pattern Formation*, Phys. Rev. E **48**, 2699 (1993).